Raman spectroscopic study of the uranyl mineral pseudojohannite $Cu_{6.5}[(UO_2)_4O_4(SO_4)_2]_2(OH)_5 \cdot 25H_2O$

Ray L. Frost, [1] • Jakub Plášil, [2] Jiří Čejka, [1,2] Jiří Sejkora, [2] Eloise C. Keeffe [1]

[1] Inorganic Materials Research Program, School of Physical and Chemical Sciences, Queensland University of Technology, GPO Box 2434, Brisbane Queensland 4001, Australia.

[2] National Museum, Václavské náměstí 68, CZ-115 79 Praha 1, Czech Republic.

Abstract

Raman spectra of pseudojohannite were studied and related to the structure of the mineral. Observed bands were assigned to the stretching and bending vibrations of $(UO_2)^{2+}$ and $(SO_4)^{2-}$ units and of water molecules. The published formula of pseudojohannite is $Cu_{6.5}(UO_2)_8[O_8](OH)_5[(SO_4)_4]\cdot 25H_2O$; however Raman spectroscopy does not detect any hydroxyl units. Raman bands at 805 and 810 cm^{-1} are assigned to $(UO_2)^{2+}$ stretching modes. The Raman bands at 1017 and 1100 cm^{-1} are assigned to the $(SO_4)^{2-}$ symmetric and antisymmetric stretching vibrations. The three Raman bands at 423, 465 and 496 cm^{-1} are assigned to the $(SO_4)^{2-}$ ν_2 bending modes. The bands at 210 and 279 cm^{-1} are assigned to the doubly degenerate ν_2 bending vibration of the $(UO_2)^{2+}$ units. U-O bond lengths in uranyl and O-H…O hydrogen bond lengths were calculated from the Raman and infrared spectra.

Keywords: pseudojohannite, mineral, uranyl, sulfate, molecular water, hydroxyls, Raman spectroscopy, U-O bond lengths, hydrogen bonds, O-H…O bond lengths

Introduction

Uranyl sulphates from a group of secondary uranyl minerals typically occurring close to actively oxidizing uraninite and sulphide minerals [1-3], inclusive e.g. uranopilite, jáchymovite, johannite, deliensite and zippeite group minerals. According to Burns et al. [3], uranyl sulfate solid state and solution chemistry plays important role in the uranyl chemistry, mineralogy, geochemistry and environmental chemistry with regard to uranium(VI) migration in natural waters and to spent nuclear fuel problems. These compounds may also be significant products of the alteration of nuclear waste in a geologic repository, owing to the presence of sulfur as an impurity in steel used to construct canisters [4]. Uranyl sulfates usually occur as admixture of species consisting of fine grained mats and coatings, making their characterization difficult [1].

Zippeite-group minerals, which may contain various low-valence (M^+, M^{2+}) cations, are among the most common uranyl sulfates in nature. The natural and

• Author to whom correspondence should be addressed (r.frost@qut.edu.au)

synthetic zippeites show therefore a wide range of compositions. Characteristic feature of zippeites is their very similar uranyl sulfate sheet topology $[(UO_2)_2(SO_4)(O)_x(OH)_{2-x}]$ with practically always UO_2/SO_4 molar ratio close to 2. The topology of the zippeite sheet thus is compatible with a wide range of interlayer configurations and water molecules contents [5,6]. A zippeite-type mineral having the proposed composition $K_{0.6}(H_3O)_{0.4}[(UO_2)_6(SO_4)_3(OH)_7].8H_2O$, was recently described by Frost et al. [7,8]. Relatively low contents of divalent cations (Mg, Ca, Fe), found in the studied sample, were omitted and the charge balance between the sheets and the interlayer was solved by inclusion of hydroxonium cations in the formula. The presence of hydroxonium was supported by Raman and infrared spectra. Recent paper by Peeters et al. [5] and recently made available thesis by McCollam [6] prove the presence of monovalent and divalent cations together contained in crystal structures of some synthetic and natural zippeites. It could be therefore inferred that such divalent cations may be present in the zippeite-type mineral studied and should be therefore included in the crystal structure and chemical formula of this phase described by Frost et al. [7,8]. As far as we know the crystal structural analysis has been not available as yet for natural zippeite (K-zippeite). However, X-ray single crystal structure of marecottite, $Mg_3(H_2O)_{18}[(UO_2)_4O_3(OH)(SO_4)_2]_2.10H_2O$ and magnesium-zippeite, $Mg(H_2O)_{3.5}[(UO_2)_2(SO_4)O_2]$ [9], and partial structure of pseudojohannite, $Cu_{6.5}[(UO_2)_4O_4(SO_4)_2]_2.25H_2O$ [10] have been published. Spicyn et al. [11] first presented X-ray single crystal structure of synthetic Zn-zippeite, $Zn_3[(UO_2)_6(SO_4)_3(OH)_{12}].4.5H_2O$, which may be also written as $Zn[(UO_2)_2(SO_4)(OH)_4].1.5H_2O$.

Unit cell parameters, infrared spectra and thermal analysis of some synthetic zippeites were shortly described by Čejka and Sejkora [12,13] and reviewed by Čejka [14]. The structures of synthetic zippeites studied by Burns et al. [4] contain topologically identical sheets of uranyl pentagonal dipyramidal coordination polyhedra and sulfate tetrahedra, however, the symmetry of the uranyl sulfate sheets, as well as their compositional details, are not identical for all synthetic zippeite-type compounds studied by Burns et al. [4]. The uranyl sulfate sheets contain three types of oxygen ligands: oxygens of uranyls, oxygens that are shared between uranyl pentagonal dipyramids, and oxygens (O, OH) that are bonded to three hexavalent uranium cations. Each structure contains the zippeite-type sheet topology consisting of chains of edge-sharing uranyl pentagonal dipyramids that are cross-linked by vertex sharing with sulfate tetrahedra, although the compositional details of the sheet are varied. The interlayer configurations are diverse, and are related to the bonding requirements of the sheets [4,15-17]. Different arrangements in the interlayers result in different unit cells and space groups [9]. Infrared spectra of uranyl sulfate minerals including zippeites were reviewed by Čejka [14] [references therein], [13], infrared and Raman spectra by Čejka [18] [references therein]. Raman spectra of some zippeites were studied by Frost et al. [7,8,19].

Pseudojohannite, triclinic $Cu_{6.5}[(UO_2)_4O_4(SO_4)_2]_2(OH)_5.25H_2O$, is formed as one of alteration product of strongly weathered uraninite containing pyrite, tennatite and chalcopyrite. It occurs at Jáchymov, Krušné hory Mts., the Czech Republic, in association with johannite, uranopilite and gypsum [20,21]. It was also found at the hydrothermal uranium deposit La Creusaz, the Aiguilles Rouges massif in the Western Swiss Alps (Switzerland) and at Musonoi near Kolwezi (Shaba, Congo).

Chemical composition and formula, X-ray powder pattern and unit-cell parameters, infrared spectrum and thermal analysis of pseudojohannite were described and interpreted by Brugger et al. [10]. Crystal structure of pseudojohannite was solved by high resolution powder diffraction with a synchrotron technique. However, only positions of U and S atoms were localized, positions of Cu, O and H were not determined [10]. Pseudojohannite contains zippeite-type sheets in its structure and illustrates the structural complexity of zippeite-group minerals containing divalent cations, which have diverse arrangements in the interlayer [10]. Pseudojohannite similarly as johannite may be understood as a product of hydrolysis from the solutions formed during hydration-oxidation weathering of copper sulfides and uraninite and containing corresponding Cu^{2+} and $(SO_4)^{2-}$ ions.

The aim of this paper is to report the Raman spectra of pseudojohannite and their comparison with published infrared spectrum together with inferring some relations to the crystal chemistry of pseudojohannite and the zippeite-type minerals. The paper follows the systematic research on Raman and infrared spectroscopy of secondary minerals containing oxy-anions formed in oxidation zone, inclusive uranyl minerals.

Experimental

Mineral

The studied sample of the mineral pseudojohannite was found at the vein Červená, Rovnost shaft (level of Daniel adit), Jáchymov ore district, the Krušné hory Mountains, northern Bohemia, Czech Republic, and is deposited in the mineralogical collections of the National Museum Prague. The sample was analysed for phase purity by X-ray powder diffraction. No minor significant impurities were found. Its refined unit-cell parameters for triclinic space group *P*1 or *P*-1, a 10.009(3), b 10.856(3), c 13.381(4) Å, α 88.23(2)°, β 109.28(1)°, γ 90.99(2)°, V 1371.7(6) Å^3, are comparable with the data published for this mineral phase [10]. The mineral was analysed by EDX methods for chemical composition. Obtained substantial contents of Cu, U and S are in agreement with the composition of pseudojohannite [10]. The results of quantitative analyses (electron microprobe Cameca SX100, WD mode) confirmed on studied pseudojohannite sample the molar ration $(UO_2)/(SO_4) \sim 2$, observed molar ration $Cu/(SO_4)$ varies in the range 1.5 - 1.7 and thus differs from the value 1.6 given by Brugger et al. [10]. The study of the role of the content of Cu and other cations in the interlayer of the crystal structure of pseudojohannite is in progress and will be published separately later.

Raman spectroscopy

The crystals of pseudojohannite were placed and oriented on the stage of an Olympus BHSM microscope, equipped with 10x and 50x objectives and part of a Renishaw 1000 Raman microscope system, which also includes a monochromator, a filter system and a Charge Coupled Device (CCD). Further details have been published [22-30].

Results and discussion

A free uranyl, $(UO_2)^{2+}$, point symmetry $D_{\infty h}$, should exhibit three fundamental modes: the Raman active symmetric stretching vibration ν_1 (~900-750 cm^{-1}), the infrared active bending vibration ν_2 (δ) (~300-200 cm^{-1}), and the infrared active antisymmetric stretching vibration ν_3 (~1000-850 cm^{-1}). The bending mode is doubly degenerate since it occurs in two mutually perpendicular planes. The peak may split into its two components when the uranyl ion is placed in an external force field. Thus, the linear uranyl group, point symmetry $D_{\infty h}$, has four normal vibrations, but only three fundamentals. The Raman active ν_1 $(UO_2)^{2+}$ appears in the infrared spectrum only in the case of substantial symmetry lowering. A lowering of symmetry ($D_{\infty h} \Rightarrow C_{\infty v}$, C_{2v} or C_s causes both the activation of all three fundamentals in the infrared and Raman spectra and the activation of their overtones and combination vibrations [14]. The doubly degenerate ν_2 (δ) $(UO_2)^{2+}$ bending vibration is infrared active, and a decrease of symmetry can cause splitting of this vibration into two infrared and Raman active components. Coincidences between uranyl bending vibrations and U-O_{ligand} vibrations were observed in some uranyl synthetic compounds and minerals [14].

Free $(SO_4)^{2-}$ anion is characterized by tetrahedral T_d symmetry. There are 9 normal vibrations characterized by four fundamental distinguishable modes of vibration, two of which are infrared and all are Raman active. Because of the Td symmetry lowering, all $(SO_4)^{2-}$ vibrations may be infrared and Raman active, and the doubly degenerate ν_2 $(SO_4)^{2-}$ bending vibrations, the triply degenerate antisymmetric stretching vibrations ν_3 $(SO_4)^{2-}$ and the triply degenerate bending vibrations ν_4 $(SO_4)^{2-}$ split. Raman and infrared bands assigned to the ν_3 $(SO_4)^{2-}$ are located in the region 1280-1040 cm^{-1}, bands attributed to the ν_1 symmetric stretching vibrations $(SO_4)^{-1}$ in 1020-950 cm^{-1}, and bands assigned to the ν_4 $(SO_4)^{2-}$ and ν_2 $(SO_4)^{2-}$ bending vibration in 680-560 cm^{-1} and 560-350 cm^{-1}, respectively. As in the case of the $(UO_2)^{2+}$ stretching vibrations, some overlap or coincidence of the $(SO_4)^{2-}$ stretching vibrations and δ U-OH bending is possible. Bands connected with libration modes of water molecules may coincide especially with bands attributed to the $(SO_4)^{2-}$ bending vibrations.

Raman spectroscopy

The Raman spectrum of pseudojohannite in the 600 to 1200 cm^{-1} region is displayed in Figure 1. Three overlapping bands are observed at 755, 805 and 810 cm^{-1}. The two bands at 805 and 810 cm^{-1} are attributed to the ν_1 symmetric stretching modes of the $(UO_2)^{2+}$ units. In the infrared spectrum published by Brugger et al. a weak infrared band at 831 cm^{-1} was interpreted as the ν_1 symmetric stretching mode of $(UO_2)^{2+}$ units. There is such a large difference between the position of the Raman band and the infrared band as published by Brugger. A possible assignment may be to water librational modes of very strongly bonded water.

However, according to Bartlett and Cooney [31], U-O bond lengths in uranyls are 1.804/874, 1.780/831, 1.800/810 and 1.806/805 Å/cm^{-1}. All these values are in excellent agreement with ~1.8 Å for uranyl synthetic and natural compounds

possessing uranyl pentagonal dipyramidal coordination polyhedra in their structures inclusive synthetic zippeites [4,15-17]. This interpretation need not therefore be incorrect. In the case of Na zippeite, the ν_1 $(UO_2)^{2+}$ symmetric stretching vibration was attributed to the Raman band at ~840 cm^{-1} (deconvoluted in four bands) and the infrared bands at 815 and 821 cm^{-1}. These are the reverse wavenumbers in comparison with the Raman and infrared spectra of pseudojohannite in this region.

In the infrared spectrum of johannite, a broad band is found at 795 cm^{-1} and a sharper band at 809 cm^{-1} [1] which correspond to the Raman bands of pseudojohannite in this region. Čejka [32] noted one (819-822 cm^{-1}) or two low intensity absorption bands at 832 and 821 cm^{-1}. One of the problems associated with studying broad overlapping bands in this region is the potential overlap with water librational modes or UOH deformation modes. One possibility is that the broad band at 755 cm^{-1} is a water librational mode and that the two bands at 805 and 810 cm^{-1} are probably the correct ν_1 symmetric stretching mode.

A sharp band at 1017 cm^{-1} is assigned to the ν_1 $(SO_4)^{2-}$ symmetric stretching mode. The band is highly polarized. The broad Raman band at 1100 cm^{-1} is attributed to the ν_3 $(SO_4)^{2-}$ antisymmetric stretching vibration. This band is broad and may be deconvoluted into a number of overlapping bands which may be assigned to this vibrational mode. In the infrared data of Brugger et al. a very low intensity band at 975 cm^{-1} was assigned to the ν_1 $(SO_4)^{2-}$ symmetric stretching mode. However, the assignment of the band related to this wavenumber is in excellent agreement also in comparison with some other sulfate minerals [33]. The position of this band differs considerably from that of the Raman band. Two intense infrared bands were observed by Brugger et al. at 1077 and 1151 cm^{-1} and were assigned to the ν_3 $(SO_4)^{2-}$ antisymmetric stretching vibration [10].

Serezhkina et al. (1982) observed two bands for johannite at 1012 and 1002 cm^{-1} and attributed them to the ν_1 $(SO_4)^{2-}$ [34]. The Raman spectrum of pseudojohannite is clearer with a sharp intense band at 1017 cm^{-1} attributed to the ν_1 $(SO_4)^{2-}$ symmetric stretching vibration. A comparison may be made with the equivalent Raman spectral region of johannite [35]. For johannite three Raman bands are observed at 1147, 1100 and 1090 cm^{-1} and are assigned to the $(SO_4)^{2-}$ antisymmetric stretching vibrations. In the infrared spectrum of johannite, two bands are observed at 1145 and 1086 cm^{-1}. Serezhkina et al. (1982) attributed bands at 1227, 1160, 1140, 1070 and 1037 to the ν_3 $(SO_4)^{2-}$. In the infrared spectrum of johannite, Čejka et al. [31] proposed *that* the symmetry of the $(SO_4)^{2-}$ anion must be of C_1 symmetry. If this is so then the ν_1 and ν_2 bands become infrared active. In this work on pseudojohannite no infrared band equivalent to the symmetric stretching mode at 1017 cm^{-1} is observed. Thus it is suggested that higher site symmetry C_{3v} is possible. The fact that only a single asymmetric band at 1100 cm^{-1} supports this concept. The infrared spectra of johannite as reported by Čejka [14] show that bands in the $(SO_4)^{2-}$ symmetric stretching region may be but need not be observed [32]. Similarly no IR bands of pseudojohannite were found in our infrared spectrum in this position which could be attributed to this vibration although a very weak shoulder at 1041 cm^{-1} was observed

The Raman spectrum of pseudojohannite in the 100 to 600 cm^{-1} region is reported in Figure 2. Raman bands are observed at 423, 465 and 496 cm^{-1}. An

additional low intensity band is observed at 539 cm^{-1}. The two bands at 465 and 496 cm^{-1} may possibly be assigned to the ν_4 bending vibration of the $(SO_4)^{2-}$ units. The positions of these bands are low for $(SO_4)^{2-}$ ν_4 bending modes. Another assignment would be to $(SO_4)^{2-}$ ν_2 bending modes, in which case the ν_4 bending modes are not observed. Brugger et al. [10] reported infrared bands at 583, 625 and 674 cm^{-1} and assigned these bands to the ν_4 bending vibration of the $(SO_4)^{2-}$ units. Infrared bands attributable to ν_2 bending modes were observed at 475 and 497 cm^{-1}.

A comparison may be made with the Raman spectrum of johannite [35]. In the Raman spectrum of johannite, a strong band is observed at 539 cm^{-1} and is assigned to the triply degenerate ν_4 bending vibration of the $(SO_4)^{2-}$ units. . In the infrared spectrum of johannite two absorption bands are observed at 619 and 605 cm^{-1} and may be assigned to this vibrational mode. Čejka [14] found absorption band at 619 cm^{-1} which is in good agreement with this work, and Serezhkina et al. [34] found four bands at 642, 611, 605 and 595 cm^{-1} and assigned these bands to the ν_4 $(SO_4)^{2-}$ bending modes. Serezhkina et al. [34] assume that theoretically should but need not be observed in the infrared spectrum of synthetic johannite 4 bands (ν_1), 8 bands (ν_2), 12 bands (ν_3) and 12 bands (ν_4). The sharp band observed at 423 cm^{-1} is ν_2 bending vibration of the $(SO_4)^{2-}$ units. Two bands are observed in the Raman spectrum of johannite at 481 and 384 cm^{-1}. These bands are band separated into bands at 469, 425 and 388 cm^{-1} at 77 K. These bands are assigned to the ν_2 bending modes of the $(SO_4)^{2-}$ units. Čejka found bands at 422 and 384 cm^{-1} in the infrared absorption spectra of johannite [32].

In the Raman spectrum of the low wavenumber region of pseudojohannite, a significant number of intense bands are observed (Figure 2). Bands are observed at 151, 162, 210 and 279 cm^{-1}. The two higher wavenumber bands at 210 and 279 cm^{-1} are assigned to the doubly degenerate ν_2 bending vibration of the $(UO_2)^{2+}$ units. A comparison may be made with the position of bands for johannite [32,35]. In the infrared spectrum of johannite Čejka assigned the two bands at 257 and 216 cm^{-1} to the doubly degenerate ν_2 bending vibration of the $(UO_2)^{2+}$ units. The two Raman bands for johannite at 277 and 205 cm^{-1} fits well with this observation. However there are significant differences between the infrared spectrum in the low wavenumber region as published by Čejka and the Raman spectrum of johannite. An additional low intensity band is observed for pseudojohannite at around 330 cm^{-1}. This band is ascribed to CuO stretching vibrations. There is an intense additional band at 302 cm^{-1} of johannite, which shows additional intensity at 77 K. It is proposed that this band is a CuO stretching vibration.

The Raman spectrum of pseudojohannite in the 1200 to 1800 cm^{-1} region is shown in Figure 3. Bands in this spectral region are of very low intensity. This is not unexpected as water is a very poor Raman scatterer and the band observed at 1625 cm^{-1} is assigned to the δ water bending mode. A very low intensity band is observed at 1675 cm^{-1} and is assigned to the δ water bending mode of very strongly hydrogen bonded water molecules. In the infrared spectrum reported by Brugger et al. [10] two bands were observed at 1627 and 1665 cm^{-1} and were assigned to water HOH bending modes. The position of the Raman bands are complemented well with the infrared bands published by Brugger et al. [10]. The two Raman bands observed at 1333 and 1554 cm^{-1} are assigned to the UOH deformation modes. Such low intensity bands were observed at 1390 and 1457 cm^{-1} in the infrared spectrum of Brugger et al.

The Raman spectrum of pseudojohannite in the 3000 to 3700 cm^{-1} region is reported in Figure 4. Three overlapping bands are observed at 3226, 3353 and 3483 cm^{-1}. The bands are assigned to water stretching vibrations. For the mineral johannite, four Raman bands were observed at 3593, 3523, 3387 and 3234 cm^{-1}. In the infrared spectrum of johannite four bands were found at 3589, 3518, 3389 and 3205 cm^{-1}. In the Raman and infrared spectra of johannite, the first two bands were assigned to OH units and the second two bands to water units. In the structure of johannite there are two independent water units and two independent (OH) units (Fig. 5). Hence the observation of the four Raman bands is in harmony with the structure of the mineral. It is concluded that in this spectral region the spectrum of pseudojohannite is very different from that of johannite. This is not unexpected as the structure of pseudojohannite is very different from johannite. Uranyl anion sheet topology of pseudojohannite, i.e. zippeite topology, and its structure differ from those of johannite. No bands attributable to OH stretching vibrations are observed. Brugger et al. reported the infrared spectrum of pseudojohannite [10]. Infrared bands were observed at 3200, 3453, 3375, 3310 and 3200 cm^{-1}. These bands were assigned to water stretching vibrations and the stretching vibrations of hydroxyl units. These authors also reported the thermogravimetric and differential thermal analysis of pseudojohannite [10].

Studies have shown a strong correlation between ν OH stretching frequencies and both O···O bond distances and H···O hydrogen bond distances. Libowitzky based upon the hydroxyl stretching frequencies as determined by infrared spectroscopy, showed that a regression function can be employed relating the above correlations with regression coefficients better than 0.96 [36]. The function is described as: $\nu_1 = (3592 - 304) \times 109^{\frac{-d(O-O)}{0.1321}}$ cm^{-1}. The two water stretching vibrations at 3226 and 3353 cm^{-1} provide estimations of the hydrogen bond distances of 2.713 and 2.769 Å. The OH stretching vibrations of the hydroxyl units at 3483 cm^{-1} gives an estimation of hydrogen bond distance of 2.873 Å. The use of Raman data instead of the infrared data would provide similar values for the estimation of the hydrogen bond distances. The results of this analysis show that the hydroxyl units are at long distances from the nearest oxygen and that the water molecules are at significantly closer distances to the nearest oxygen. Such a conclusion fits well with the known partial structure of pseudojohannite in which the sulphates link with water units to form a semi-layered structure if this interpretation is correct. According to Libowitzky [37], observed O-H…O hydrogen bond lengths are 2.59-3.48 Å(H_2O) and 2.46-3.69 Å. Some overlapping of corresponding bands attributable to ν OH stretching vibrations of water molecules and hydroxyl ions may be therefore expected.

Conclusions

Raman spectroscopy has enabled a study of the uranyl sulphate mineral known as pseudojohannite. Whereas infrared spectroscopy provides a complex spectral

profile as a result of overlapping bands making the assignment of bands difficult, Raman spectroscopy enables better band separation with bandwidths being significantly smaller. Further Raman spectroscopy provides information on the symmetric stretching modes whereas infrared spectroscopy may show these bands providing the symmetry of the vibration species is lowered to enable the modes to become Raman active. Even then the infrared band may be lost in the complex spectral profile as often happens with secondary uranyl minerals. Another difficulty which Raman spectroscopy can help to overcome is the overlap of bands which arise from the position of bands from different vibrating species occurring at the same or similar positions.

Acknowledgements

The financial and infra-structure support of the Queensland University of Technology Inorganic Materials Research Program of the School of Physical and Chemical Sciences is gratefully acknowledged. The Australian Research Council (ARC) is thanked for funding. This work was also supported by Ministry of Culture of the Czech Republic (MK00002327201) to Jiří Sejkora and Grant Agency of Charles University in Prague (17008/2008) to Jakub Plášil.

References

1. Frondel, C. Systematic mineralogy of uranium and thorium.; U.S. Geol. Survey Bull., 1958.
2. Smith, DK *Uranium mineralogy, In Uranium geochemistry, mineralogy, geology, exploration and resources*; The Institution of Mining and Metallurgy London, 1984.
3. Finch, R, Murakami, T. *Reviews in Mineralogy* 1999**; 38**: 91.
4. Burns, PC, Deely, KM, Hayden, LA. *Canadian Mineralogist* 2003**; 41**: 687.
5. Peeters, OM, Vochten, R, Blaton, N. *Canadian Mineralogist* 2008**; 46**: 173.
6. McCollam, BE. *Zippeites: chemical characterization and powder X-ray diffraction studies of synthetic and natural samples*, University of Notre Dame 2004.
7. Frost, RL, Cejka, J, Ayoko, GA, Weier, ML. *Journal of Raman Spectroscopy* 2007**; 38**: 1311.
8. Frost, RL, Cejka, J, Bostrom, T, Weier, M, Martens, W. *Spectrochimica Acta, Part A: Molecular and Biomolecular Spectroscopy* 2007**; 67A**: 1220.
9. Brugger, J, Burns, PC, Meisser, N. *American Mineralogist* 2003**; 88**: 676.
10. Brugger, J, Wallwork, KS, Meisser, N, Pring, A, Ondrus, P, Cejka, J. *American Mineralogist* 2006**; 91**: 929.
11. Spitsyn, VI, Kovba, LM, Tabachenko, VV, Tabachenko, NV, Mikhaylov, YN. *Izv. Akad. Nauk SSSR, Ser. Khim.* 1982**; (in Russian)**: 807.
12. Čejka, J, Sejkora, J. *Mineralogy, geochemistry and the environment* 1994**; Proc. 6th Mineral Seminar**: 28.
13. Cejka, J, Sejkora, J, Mrazek, Z, Urbanec, Z, Jarchovsky, T. *Neues Jahrbuch fuer Mineralogie, Abhandlungen* 1996**; 170**: 155.
14. Cejka, J. *Reviews in Mineralogy* 1999**; 38**: 521.
15. Burns, PC. *Reviews in Mineralogy* 1999**; 38**: 23.
16. Burns, PC, Ewing, RC, Hawthorne, FC. *Canadian Mineralogist* 1997**; 35**: 1551.
17. Burns, PC, Miller, ML, Ewing, RC. *Canadian Mineralogist* 1996**; 34**: 845.
18. Sejkora, J, Cejka, J, Srein, V. *Journal of Geosciences* 2007**; 52**: 199.
19. Frost, RL, Weier, ML, Bostrom, T, Cejka, J, Martens, W. *Neues Jahrbuch fuer Mineralogie, Abhandlungen* 2005**; 181**: 271.
20. Ondrus, P, Veselovsky, F, Gabasova, A, Drabek, M, Dobes, P, Maly, K, Hlousek, J, Sejkora, J. *Journal of the Czech Geological Society* 2003**; 48**: 157.
21. Ondrus, P, Veselovsky, F, Hlousek, J, Skala, R, Vavrin, I, Fryda, J, Cejka, J, Gabasova, A. *Journal of the Czech Geological Society* 1997**; 42**: 3.
22. Frost, RL, Cejka, J, Ayoko, G. *Journal of Raman Spectroscopy* 2008**; 39**: 495.
23. Frost, RL, Cejka, J, Ayoko, GA, Dickfos, MJ. *Journal of Raman Spectroscopy* 2008**; 39**: 374.
24. Frost, RL, Cejka, J, Dickfos, MJ. *Journal of Raman Spectroscopy* 2008**; 39**: 779.
25. Frost, RL, Dickfos, MJ, Cejka, J. *Journal of Raman Spectroscopy* 2008**; 39**: 582.
26. Frost, RL, Hales, MC, Wain, DL. *Journal of Raman Spectroscopy* 2008**; 39**: 108.
27. Frost, RL, Keeffe, EC. *Journal of Raman Spectroscopy* 2008**; in press**.
28. Frost, RL, Locke, A, Martens, WN. *Journal of Raman Spectroscopy* 2008**; 39**: 901.

29. Frost, RL, Reddy, BJ, Dickfos, MJ. *Journal of Raman Spectroscopy* 2008**; 39**: 909.
30. Palmer, SJ, Frost, RL, Ayoko, G, Nguyen, T. *Journal of Raman Spectroscopy* 2008**; 39**: 395.
31. Bartlett, JR, Cooney, RP. *J. Mol. Struct.* 1989**; 193**: 295.
32. Cejka, J, Urbanec, Z, Cejka, J, Jr., Mrazek, Z. *Neues Jahrbuch fuer Mineralogie, Abhandlungen* 1988**; 159**: 297.
33. Lane, MD. *American Mineralogist* 2007**; 92**: 1.
34. Serezhkina, AN, Serezhkin, VN, Soldatkina, MA. *Zhurnal Neorganicheskoy Khimii* 1982**; 27**: 1750.
35. Frost, RL, Erickson, KL, Cejka, J, Reddy, BJ. *Spectrochimica Acta, Part A: Molecular and Biomolecular Spectroscopy* 2005**; 61A**: 2702.
36. Libowitsky, E. *Monatschefte fÜr chemie* 1999**; 130**: 1047.
37. Libowitzky, E. *Monatshefte fuer Chemie* 1999**; 130**: 1047.

List of Figures

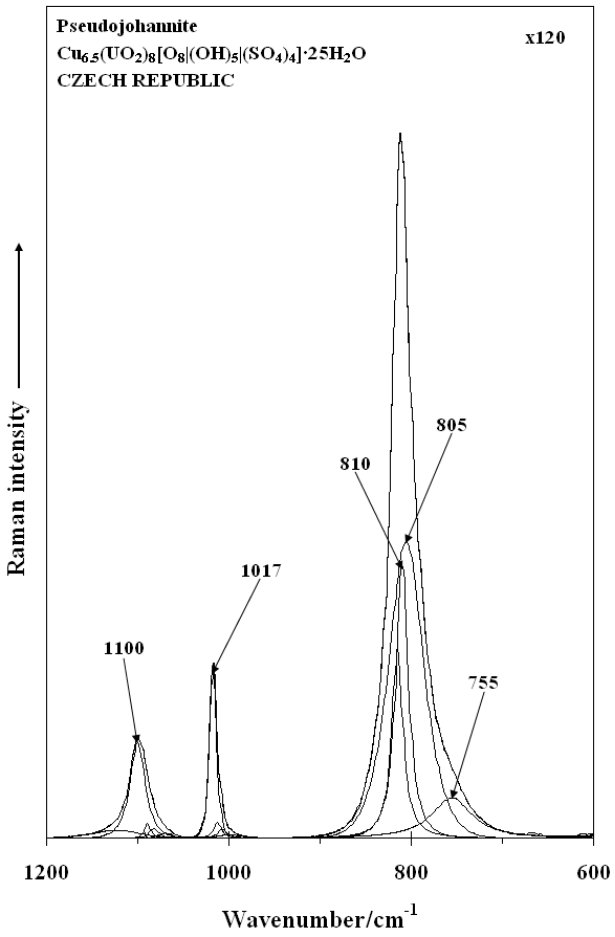
Pseudojohannite
Cu6.5(UO2)8[O8|(OH)5|(SO4)4]·25H2O
CZECH REPUBLIC
x120
Raman intensity
1100
1017
810
805
755
1200
1000
800
600
Wavenumber/cm-1

Figure 1

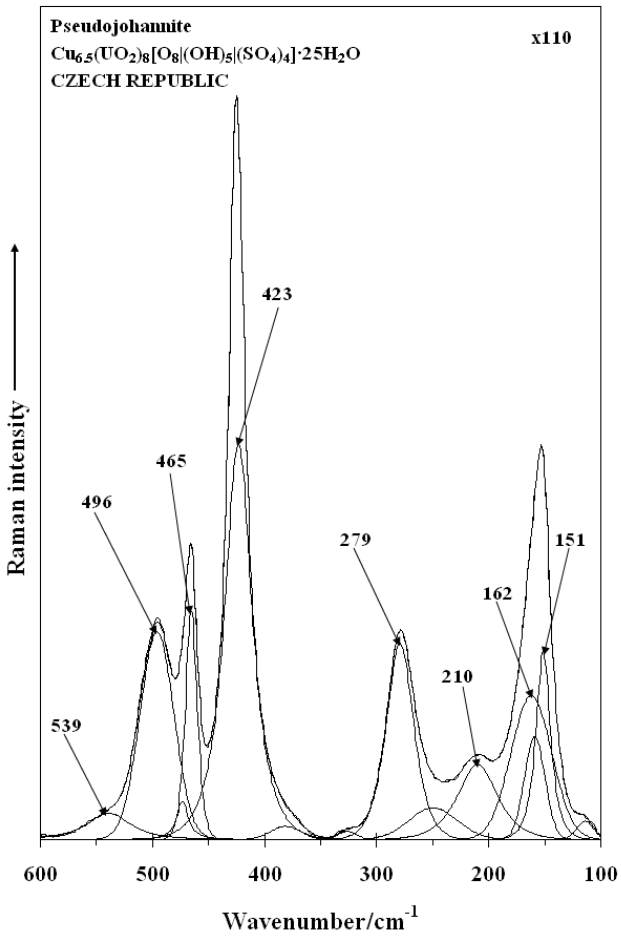
Pseudojohannite
Cu6.5(UO2)8[O8|(OH)5|(SO4)4]·25H2O
CZECH REPUBLIC
x110
Raman intensity
423
465
496
279
151
162
210
539
600
500
400
300
200
100
Wavenumber/cm-1

Figure 2

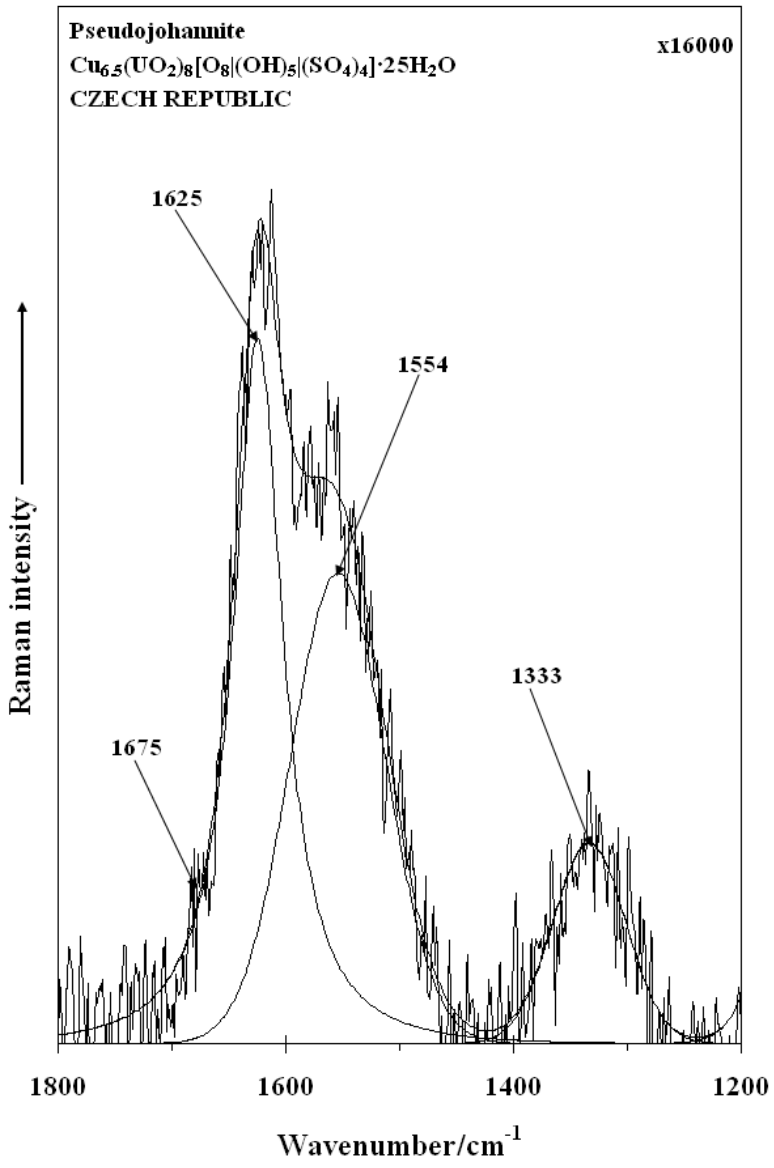
Pseudojohannite
$Cu_{6.5}(UO_2)_8[O_8|(OH)_5|(SO_4)_4]\cdot 25H_2O$
CZECH REPUBLIC
x16000
1625
1554
1333
1675
Raman intensity
1800
1600
1400
1200
Wavenumber/cm^{-1}

Figure 3

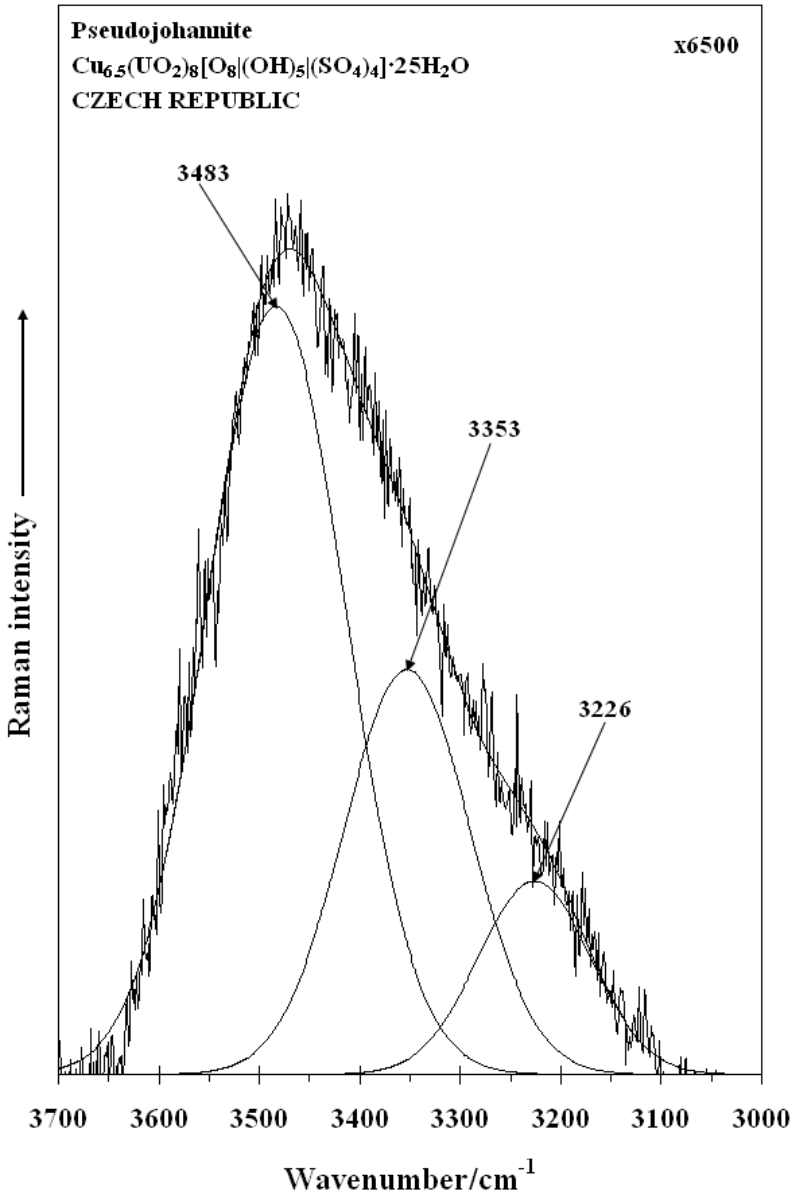
Pseudojohannite
$Cu_{6.5}(UO_2)_8[O_8|(OH)_5|(SO_4)_4]\cdot 25H_2O$
CZECH REPUBLIC
x6500
3483
3353
3226
Raman intensity
3700
3600
3500
3400
3300
3200
3100
3000
Wavenumber/cm^{-1}

Figure 4

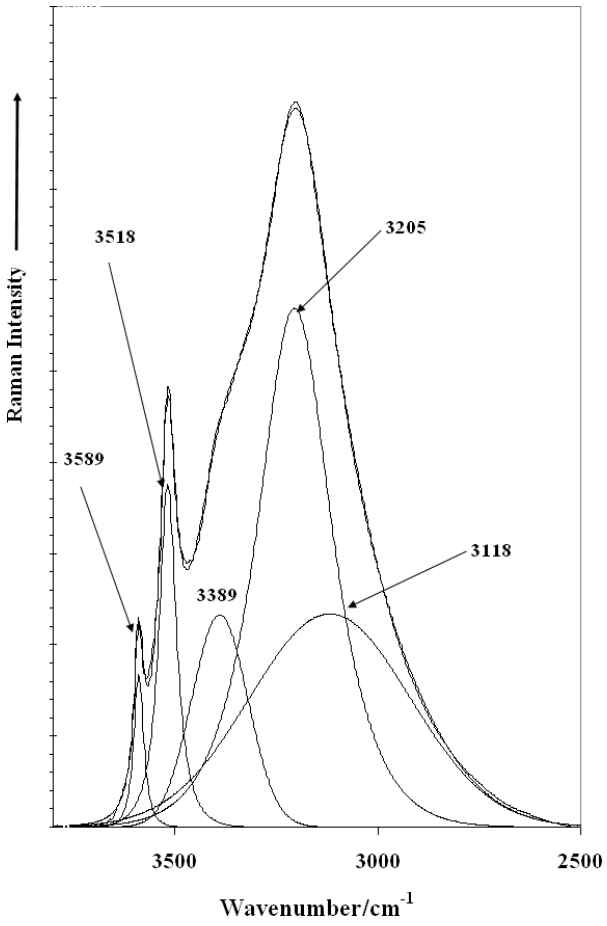

Figure 5 RS-johannite